Does a Large Array Aperture Pay Off in Line-Of-Sight Massive MIMO?

Stefan Pratschner*†, Erich Zöchmann*†‡, Herbert Groll†, Sebastian Caban*†, Stefan Schwarz*† and Markus Rupp†
‡Department of Radio Electronics, Brno Univeristy of Technology, Czech Republic
*Christian Doppler Laboratory for Dependable Wireless Connectivity for the Society in Motion
†Institute of Telecommunications, TU Wien, Austria, Email: stefan.pratschner@tuwien.ac.at

***Abstract*—Massive multiple-input multiple-output (MIMO) is considered a promising PHY scheme for future mobile communications systems. As it aims to serve many users simultaneously via spatial multiplexing, a high number of antennas at the base station is required. Since this leads to implementation issues in terms of hardware and signal processing complexity, efforts to increase the system performance for a given number of antennas are worthwhile. In this contribution, we investigate the gain in achievable downlink sum spectral efficiency (SE) of a massive MIMO system due to increased array apertures. We compare different antenna array configurations and precoder normalization strategies for maximum ratio transmission precoding and regularized zero forcing precoding. By quantifying the increase in achievable SE that is obtained when increasing the inter-antenna spacing of a linear array, we show that it hardly pays off to increase the array aperture.**

***Index Terms*—antenna array, large array, massive MIMO, multi-user MIMO**

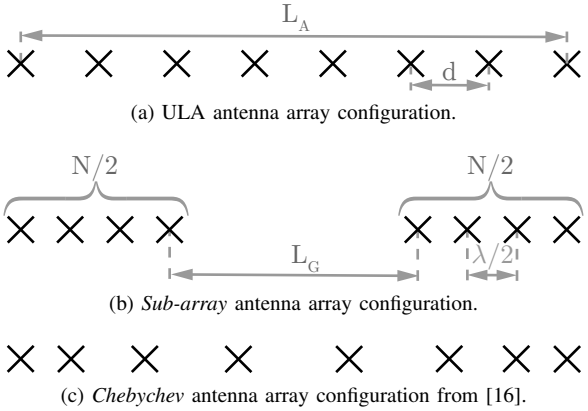

(a) ULA antenna array configuration.

(b) *Sub-array* antenna array configuration.

(c) *Chebychev* antenna array configuration from [16].

Fig. 1. Antenna array configurations. The total array aperture (length) and the total number of antennas N are equal for all cases.

I. Introduction

Massive multiple-input multiple-output (MIMO) is considered a key physical layer scheme to achieve enhanced data rates in future mobile communications networks [1]. As a multi-user MIMO scheme, it aims to serve many users on the same time-frequency resources while reducing the amount of fading due to the employment of a high number of antennas. In order to achieve the promised spatial multiplexing gains, a key aspect is achieving orthogonality of user channels. While it is trivial to achieve low inter-user correlation (IUC) to spatially separate users in a rich fading environment, narrow beams are necessary to distinguish closely located users in a line of sight (LOS) scenario. Although an array's beam width decreases when the number of antennas is increased, massive MIMO systems with high numbers of antennas suffer from signal processing and hardware complexity issues [2]. An alternative way to enhance user separability is to increase the antenna array aperture while keeping the number of antenna elements constant. The increased aperture size is achieved by enlarging the inter-antenna spacing. This strategy, however, does not only lead to sharp beams, but also results in grating lobes (or beamforming ambiguity) due to spatial under-sampling. A user located at the direction of a grating lobe suffers from strong interference, leading to a deteriorated sum spectral efficiency (SE). Due to these two competing effects, it is not a priori clear if or how beneficial an increased array aperture is for massive MIMO system performance.

Many works consider the correlation of user channels in multi-user MIMO systems, analytically as well as experimentally [3]–[9]. Deployment of sub arrays for user separation is considered in [3]. Selecting sub arrays from a large planar array is investigated in [8] while base station antenna spacing is considered in [10]. The impact of small antenna spacings on massive MIMO performance is analyzed in [11]–[15]. Authors of [11] show that there is a limited benefit in increasing the number of antennas in a fixed space for the performance of massive MIMO systems. The impact of antenna spacing and non-equidistant antenna arrays for LOS massive MIMO is investigated in [16]. Since for antenna spacings below 0.5λ, λ denoting the wavelength, the effects of mutual coupling become dominant and lead to deteriorated performance, see [17] and [18], we do not consider smaller antenna spacings.

Contribution: We investigate the influence of antenna array aperture size on the achievable sum SE in a massive MIMO downlink LOS scenario. The assumption of pure LOS, corresponding to free space propagation, renders our results

This work has been funded by the Christian Doppler Laboratory for Dependable Wireless Connectivity for the Society in Motion. The financial support by the Austrian Federal Ministry for Digital and Economic Affairs and the National Foundation for Research, Technology and Development is gratefully acknowledged. The research described in this paper was co-financed by the Czech Science Foundation, Project No. 17-18675S Future transceiver techniques for the society in motion.

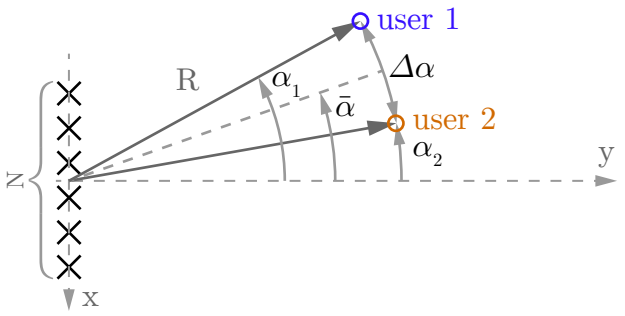

Fig. 2. Geometry for IUC analysis for the case of two users.

representative for environments in which the LOS component is dominant. By comparing three different linear array configurations, we show the influence of the antenna array pattern on the IUC and the achievable SE. We consider an equidistantly spaced uniform linear array (ULA), an antenna array configuration from [16] and the deployment of two sub-arrays. We quantify improvements in sum SE via simulation results for maximum ratio transmission (MRT) precoding and regularized zero forcing (RZF) precoding with two different power normalization methods.

II. Antenna Array Configurations

In this section, we introduce three antenna array configurations that will be employed for numerical simulations of the achievable sum SE in Section III. We analyze their antenna patterns in terms of IUC and discuss the implications on massive MIMO system performance.

We consider linear antenna arrays with isotropic elements. To analyze the IUC, we consider a setup with two users as shown in Fig. 2. A linear array with N elements is located at the origin and two users are at distance R. We assume N to be an even number. Here, the first user is at an angle of α_1 while the second user is at an angle of α_2 relative to the array's broadside direction. The angle $\Delta\alpha = \alpha_1 - \alpha_2$ describes the relative location of the two users to each other, while the angle $\overline{\alpha} = \frac{\alpha_1+\alpha_2}{2}$ describes the users' mean offset from the broadside direction.

With a far field assumption and pure LOS propagation, the channel vectors for the ULA as shown in Fig. 1a are given by

$$\mathbf{h}_q^{\mathrm{ULA}} = \left(e^{-i\frac{N}{2}kd\sin(\alpha_q)}, \ldots, e^{i\frac{N}{2}kd\sin(\alpha_q)}\right)^{\mathrm{T}} \quad q \in \{1,2\}, \quad (1)$$

where d denotes the inter-antenna spacing and $k = 2\pi/\lambda$ is the wave vector's magnitude.

To quantify the IUC, we consider the inner product of the two channels $\mathbf{h}_1$ and $\mathbf{h}_2$. This quantity is commonly employed as correlation measure of MIMO channels [6]–[8]. Inserting (1) and applying basic algebra, we obtain

$$\rho(\Delta\alpha, \overline{\alpha}) = \frac{\left|\mathbf{h}_1^{\mathrm{H}}\mathbf{h}_2\right|^2}{\|\mathbf{h}_1\|_2^2 \|\mathbf{h}_2\|_2^2} \quad (2)$$

$$= \frac{1}{N^2} \frac{\sin^2\left(Nkd\sin(\frac{\Delta\alpha}{2})\cos(\overline{\alpha})\right)}{\sin^2\left(kd\sin(\frac{\Delta\alpha}{2})\cos(\overline{\alpha})\right)}, \quad (3)$$

which is the squared array factor of a ULA [19]. As a simple measure of user separability, one may consider the first zero of $\rho(\Delta\alpha, \overline{\alpha})$ for the case $\overline{\alpha} = 0$ where user separability is best. The first zero is located at

$$\Delta\alpha^*_{\mathrm{ULA}} = 2\arcsin\left(\frac{\pi}{Nkd}\right). \quad (4)$$

This shows that the property of user separability, which is the ability to form narrow beams in a LOS environment, indeed improves with an increasing number of antennas. Furthermore, (4) demonstrates that the user separability is not only dependent on the number of antennas, but actually depends on the size or aperture Nd of the ULA.

This observation leads to the idea that the total array aperture (or length), and not the number of elements alone, is important to form narrow beams and separate closely spaced users. Therefore, we introduce a sub-array configuration as shown in Fig. 1b. The configuration consists of two ULAs of $N/2$ elements with $\lambda/2$ spacing. These two sub-arrays are separated by a gap of length L_{G}. We choose the length of the gap according to $L_{\mathrm{G}} = L_{\mathrm{A}} - \lambda/2(N-2)$ such that the sub-array configuration has the same total array length $L_{\mathrm{A}} = (N-1)d$ as the ULA configuration with antenna spacing d. Please note that for $d = \lambda/2$, the introduced *sub-array* configuration collapses to the ULA.

With the channel vectors for user $q \in \{1,2\}$

$$\mathbf{h}_q = \Big(e^{-i\left(\frac{L_{\mathrm{G}}}{2}+\left(\frac{N}{2}-1\right)\frac{\lambda}{2}\right)k\sin(\alpha_q)}, \ldots, e^{-i\frac{L_{\mathrm{G}}}{2}k\sin(\alpha_q)}, \quad (5)$$
$$e^{i\frac{L_{\mathrm{G}}}{2}k\sin(\alpha_q)}, \ldots, e^{i\left(\frac{L_{\mathrm{G}}}{2}+\left(\frac{N}{2}-1\right)\frac{\lambda}{2}\right)k\sin(\alpha_q)}\Big)^{\mathrm{T}},$$

following the same calculation steps as above, we obtain an expression for the IUC for the *sub-array* as

$$\rho(\Delta\alpha, \overline{\alpha}) = \frac{4}{N^2} \frac{\sin^2\left(\frac{N}{2}\pi\sin(\frac{\Delta\alpha}{2})\cos(\overline{\alpha})\right)}{\sin^2\left(\pi\sin(\frac{\Delta\alpha}{2})\cos(\overline{\alpha})\right)} \quad (6)$$
$$\times \cos^2\left(\left(L_{\mathrm{G}} + \frac{\lambda}{2}\left(\frac{N}{2}-1\right)\right)k\sin\left(\frac{\Delta\alpha}{2}\right)\cos(\overline{\alpha})\right).$$

In this case, the first zero for $\overline{\alpha} = 0$ is given by

$$\Delta\alpha^*_{\mathrm{sub}} = 2\arcsin\left(\frac{\pi}{2k\left(L_{\mathrm{G}} + \left(\frac{N}{2}-1\right)\frac{\lambda}{2}\right)}\right). \quad (7)$$

Comparing (4) and (7), it is straight forward to show that $\Delta\alpha^*_{\mathrm{sub}} < \Delta\alpha^*_{\mathrm{ULA}}$ for $d > \lambda/2$.

A different approach is followed in [16]. There, authors propose a non-uniform spaced linear array, where antenna element spacings are obtained via Chebyshev polynomials. This leads to an array configuration, where the element density is increased towards the ends of the array and thinned in the center of the array, as illustrated in Fig. 1c. Authors of [16] show that this antenna placement is beneficial in terms of achievable sum SE compared to an equidistant antenna spacing. We refer to this array type as *Chebychev* configuration.

Simulation results for the IUC as defined in (2) for the three introduced array configurations are shown in Fig. 3 for a user distance of $R = 60\,\mathrm{m}$. Please note that these results

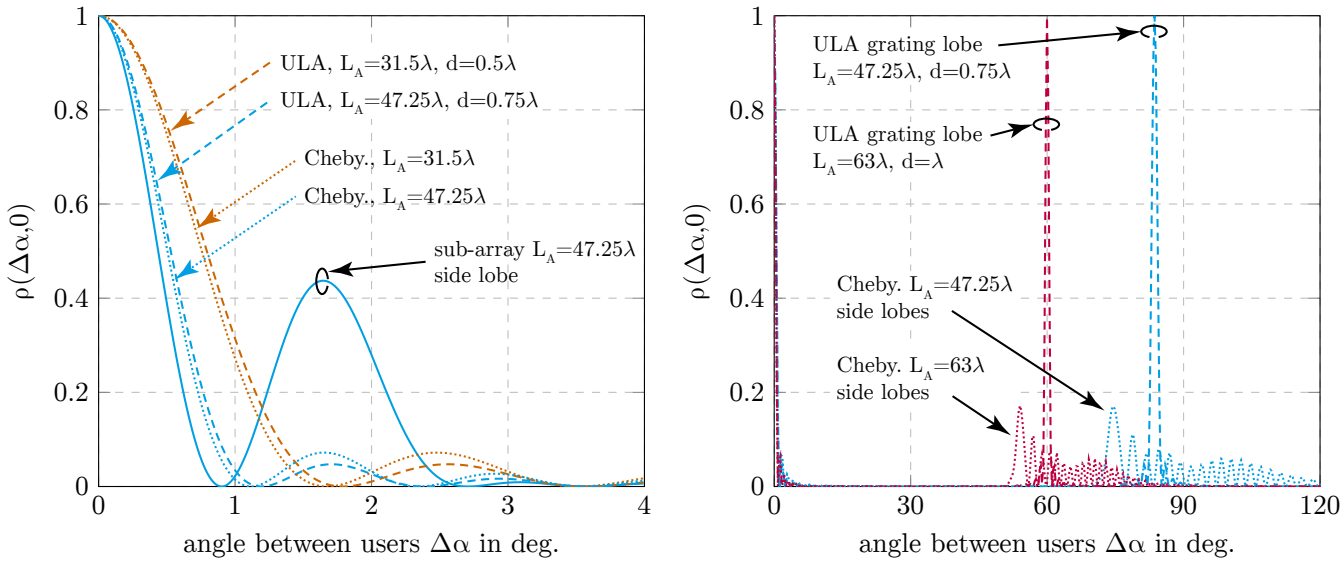

(a) Small angular region around the main lobe. The *Sub-array* configuration has side lobes close to the main lobe.

(b) Large angular region. The ULA has grating lobes while the *Chebychev* array has side lobes.

Fig. 3. IUC for different array aperture sizes and antenna array configurations with $N = 64$ and user distance $R = 60\,\text{m}$.

are obtained via numerical simulation without the simplifying assumption of planar wavefronts. Nevertheless, for the ULA and the *sub-array* configuration, the results perfectly match the analytic results obtained by (3) and (6). This verifies, as already found by others [16] that spherical wavefronts only improve separation of users with a largely different distance. A comparison to the analytically obtained results are omitted here to improve clarity of the given IUC result plot.

The width of the main beam decreases with increased array length, see Fig. 3a. In the case of a regularly spaced ULA, grating lobes occur for spacings $d > 0.5\lambda$ due to the spatial under-sampling, see Fig. 3b. Other than a side lobe, a grating lobe is a maximum in the array pattern that is as strong as the main lobe. With increased antenna spacing, the grating lobe position gets closer relative to the main lobe.

In the case of the *Chebychev* configuration, grating lobes are suppressed due to the non equidistant spacing of antennas. From Fig. 3b we see that the interference power is spread out in the *Chebychev* configuration compared to the grating lobes in the ULA case.

The antenna spacing in the *Chebychev* configuration is not uniform, resulting in a higher antenna density towards the ends of the array, see Fig. 1c. Taking this idea further, the *sub-array* configuration can be interpreted as an extreme case, where antennas at the end of the array are spaced with an inter-element distance of 0.5λ. There are no elements between these two sub-arrays, resulting in a gap. This configuration may also be interpreted as the result of an antenna selection scheme from a ULA with more antennas [20], [21]. There are no grating lobes are present between the broadside and end fire direction for the *sub-array* configuration. However, from Fig. 3a we observe side lobes close to the main beam. Therefore, this antenna array leads to decreased IUC due to the absence grating lobes. This advantage comes at the cost of side lobes close to the main beam, which lead to increased IUC for closely spaced users.

III. Simulation Results

We consider a multi-user MIMO downlink system. The vector of received signals for U users is given by

$$\mathbf{y} = \mathbf{H}^{\mathrm{H}}\mathbf{F}\mathbf{x} + \mathbf{w} \in \mathbb{C}^{U\times 1}\,, \tag{8}$$

where $\mathbf{x} \in \mathbb{C}^{U\times 1}$ is the vector of random transmit symbols, $\mathbf{F}$ is the precoding matrix and $\mathbf{w}$ is additive white Gaussian noise, that is, $\mathbf{w} \sim \mathcal{CN}\left(\mathbf{0}, \sigma_w^2\mathbf{I}_U\right)$. We employ independent transmit symbols of unit power, that is, $\mathbb{E}\left\{\mathbf{x}\mathbf{x}^{\mathrm{H}}\right\} = \mathbf{I}_U$. The channel matrix $\mathbf{H}$ is given by $\mathbf{H} = (\mathbf{h}_1, \ldots, \mathbf{h}_U)$, where column vectors are the channel vectors for each user as given by (1). We consider an MRT precoder, given by

$$\widetilde{\mathbf{F}}_{\mathrm{MRT}} = \mathbf{H}, \tag{9}$$

as well as a RZF precoding strategy, given by

$$\widetilde{\mathbf{F}}_{\mathrm{RZF}} = \mathbf{H}\left(\mathbf{H}^{\mathrm{H}}\mathbf{H} + \frac{\sigma_w^2}{P_T}\mathbf{I}_U\right)^{-1}. \tag{10}$$

Since the transmit symbols are of unit power, a sum power constraint of the form $\mathbb{E}\left\{\,\|\mathbf{F}\mathbf{x}\|_2^2\,\right\} \leq P_T$ leads to the requirement $\|\mathbf{F}\|_{\mathrm{F}}^2 \leq P_T$, where $\|\cdot\|_{\mathrm{F}}$ denotes the Frobenius norm. In this work, we consider two different ways of normalization to achieve this power constraint. An *overall* normalization, which is given by

$$\mathbf{F} = \sqrt{P_T}\frac{\widetilde{\mathbf{F}}}{\left\|\widetilde{\mathbf{F}}\right\|_{\mathrm{F}}}\,, \tag{11}$$

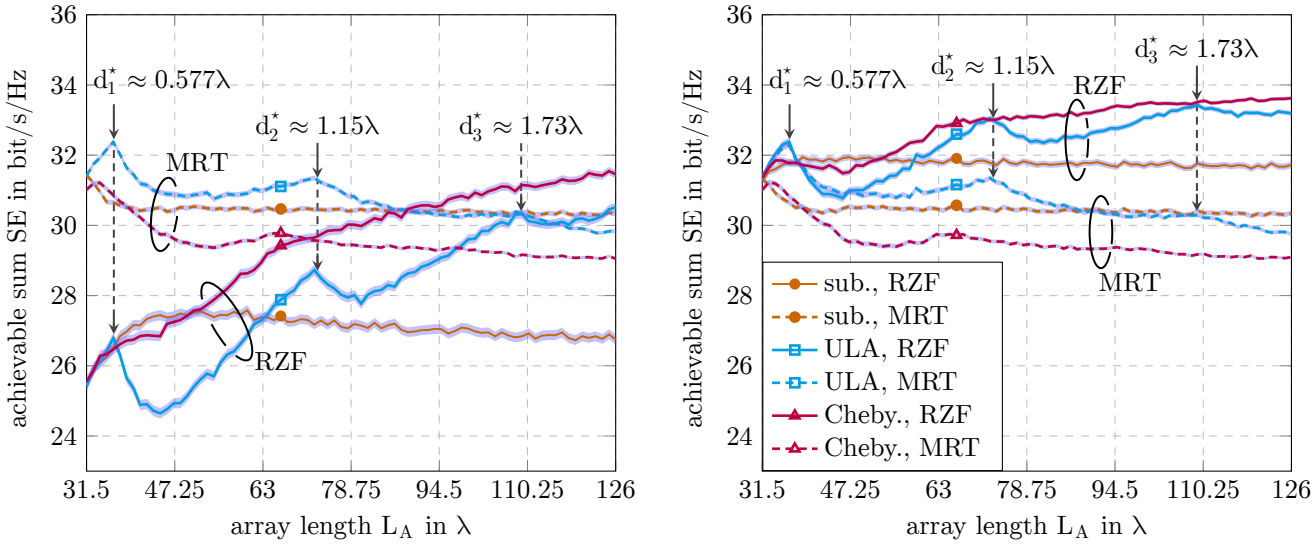

(a) *Overall* precoder normalization.

(b) *Per-user* precoder normalization.

Fig. 4. Achievable downlink sum SE with $N = 64$ assuming perfect channel knowledge. The 95% confidence regions are indicated in gray.

as well as a *per-user* normalization, which is given by

$$\mathbf{f}_u = \sqrt{\frac{P_T}{U}} \frac{\widetilde{\mathbf{f}}_u}{\left\|\widetilde{\mathbf{f}}_u\right\|_2} \quad \forall u \in \{1, \ldots, U\} \ , \tag{12}$$

where $\mathbf{f}_u$ denotes the u^{th} column of $\mathbf{F}$ and $\widetilde{\mathbf{f}}_u$ denotes the u^{th} column of $\widetilde{\mathbf{F}}$.

To obtain results for the achievable sum SE, we perform numerical simulations in a massive MIMO LOS scenario. We consider $U = 20$ users with a single antenna each at a constant distance of $R = 60\,\text{m}$ and uniformly distributed angles within a sector of $(-60°, 60°)$. This limitation of angular range relaxes the assumption of an isotropic antenna element pattern. The employed isotropic antenna elements correspond to a practical element pattern that is constant within the angular range of a sector only. As there is no minimum separation between users, they eventually have very similar angular positions. In a practical deployment, this corresponds to the case when users are located at the same angle but at different distances. The number of antennas of the antenna array is fixed to $N = 64$ and the array length L_A is varied. For our simulations we do not employ a far field assumption but employ spherical wave fronts. The signal to interference and noise ratio of user k is

$$\text{SINR}_k = \frac{\left|\left[\mathbf{H}^{\text{H}}\mathbf{F}\right]_{k,k}\right|^2}{\sum_{\substack{j=1 \\ j\neq k}}^{U} \left|\left[\mathbf{H}^{\text{H}}\mathbf{F}\right]_{k,j}\right|^2 + \sigma_w^2} \ , \tag{13}$$

where $[\mathbf{X}]_{k,j}$ denotes the entry from the k^{th} row and the j^{th} column of matrix $\mathbf{X}$. The achievable sum SE is obtained as

$$R_{\text{sum}} = \sum_{k=1}^{U} \log_2\left(1 + \text{SINR}_k\right) \ . \tag{14}$$

For a typical massive MIMO downlink scenario, we choose $P_T = \sigma_w^2 = 1$. We perform 5 000 independent realizations, that is, random draws of user positions, to obtain results for the average system performance for MRT and RZF precoding.

Results for an *overall* precoder normalization according to (11) are shown in Fig. 4a and results for a *per-user* precoder normalization according to (12) are shown in Fig. 4b. The three different introduced antenna array configurations from Fig. 1 are compared.

For the case of *overall* precoder normalization with RZF precoding, a gain in SE is obtained with increasing array length. However, as described in Section II, there are two competing effects affecting the IUC when increasing the array aperture. The width of the main lobe is reduced when increasing d which reduces the amount of IUC for closely located users. At the same time, grating lobes appear within the sector, which increases the IUC for well separated users.

The increase in achievable SE is monotonic for the *Chebychev* configuration since it effectively suppresses grating lobes. In the ULA case, the SE is also increased with larger d in general, however, this gain is not monotonic. For a ULA, the position of the n^{th} grating lobe is given by $\sin(\alpha_1) - \sin(\alpha_2) = n\frac{\lambda}{d}$ with user angles α_1 and α_2, see [19]. Thereby, we find the antenna spacing of a ULA $d_n^\star$ for which the n^{th} grating lobes start to fall into the sector, that is, the grating lobe position for $\alpha_1 = 60°$ and $\alpha_2 = -60°$. We find $d_1^\star \approx 0.577\lambda$, $d_2^\star \approx 1.155\lambda$ and $d_3^\star = 1.732\lambda$. These array sizes or antenna spacings are marked in Fig. 4. We observe a drop in SE for the ULA for antenna spacings slightly higher then spacings at which grating lobes appear within the sector due to the increase in IUC.

For the *sub-array* configuration, the gain in SE is even more pronounced compared to the *Chebychev* case until $L_A \approx 48\lambda$. In this region, there is less IUC in the *sub-array* case as there

are no grating lobes in this configuration. As there are side lobes appearing next to the main lobe, there is no more gain in SE with increased gap length as closely spaced users cannot be separated anymore. This described gain for RZF precoding, however, is not of any practical meaning, as it is outperformed by the less complex MRT precoder and a ULA with a spacing of $d_1^\star$. There is an overall loss for all array configurations in SE with increasing array length, since the MRT precoder does not mitigate the IUC.

Considering the case of *per-user* precoder normalization with RZF precoding, the gain in achievable SE is lower compared to the *overall* precoder normalization. The achievable SE is significantly impacted by situations, where users are placed close to each other. In these cases, strong correlation between user channels of two users impacts the total downlink SE via the *overall* precoder normalization. As the precoder spends the majority of power on the highly correlated users, there is less transmit power left for users with good channel conditions. Since two strongly correlated users have less impact on the sum SE in the *per-user* normalization case, there is less SE to gain by reducing the width of the main beam, that is, by increasing the array length.

The most interesting observation is the ULA performance at $d_1^\star$. Increasing the array length from $L_\mathrm{A} = (N-1)d_1^\star \approx 36.4\lambda$ to $L_\mathrm{A} = 126\lambda$ increases the achievable SE from ≈ 32.5 bit/s/Hz in the ULA case to ≈ 33.6 bit/s/Hz in the *Chebychev* case. This means that with the described simulation parameters, an increase of array length by a factor of 3.5 and deployment of non-equidistant spacing leads to a gain of $\approx 3.4\%$ in achievable sum SE with RZF precoding. A second key observation is that the SE achieved with an ULA at $d_1^\star$ and MRT precoding is almost the same as with the more complex RZF precoding.

IV. Conclusion

In this contribution, we analyze the impact of antenna array size on the achievable sum SE in a LOS downlink massive MIMO scenario. We compare three different antenna array types with MRT and RZF precoding, for an *overall* and a *per-user* power normalization. The presented results show that the gain due to increased array aperture for an *overall* precoder normalization with RZF precoding is of no practical significance, as higher SEs are achieved with the less complex MRT precoding at smaller array sizes. While an increase in achievable SE is obtained by increasing the antenna distance with a *per-user* normalization, the array size needs to be increased by a factor of 3.5 for an increase in SE of 3.4%. As the achieved SE for *per-user* precoder normalization at $d_1^\star$ is almost the same for RZF and MRT precoding, we conclude that this spacing in combination with the less complex MRT scheme is a good compromise.

References

[1] E. Björnson, E. G. Larsson, and T. L. Marzetta, "Massive MIMO: ten myths and one critical question," *IEEE Communications Magazine*, vol. 54, no. 2, pp. 114–123, Feb. 2016.

[2] L. Liang, W. Xu, and X. Dong, "Low-complexity hybrid precoding in massive multiuser MIMO systems," *IEEE Wireless Communications Letters*, vol. 3, no. 6, pp. 653–656, Dec. 2014.

[3] C.-M. Chen, V. Volskiy, A. Chiumento, L. V. der Perre, G. A. Vandenbosch, and S. Pollin, "Exploration of user separation capabilities by distributed large antenna arrays," in *IEEE Globecom Workshops*, Washington, DC, USA, 2016, pp. 1–6.

[4] J. Flordelis, F. Rusek, X. Gao, G. Dahman, O. Edfors, and F. Tufvesson, "Spatial separation of closely-located users in measured massive MIMO channels," *IEEE Access*, vol. 6, pp. 40 253–40 266, 2018.

[5] M. Z. Aslam, Y. Corre, E. Bjoernson, and Y. Lostanlen, "Massive MIMO channel performance analysis considering separation of simultaneous users," in *ITG Workshop on Smart Antennas*, Bochum, Germany, 2018, pp. 1–6.

[6] N. Czink, B. Bandemer, G. Vazquez-Vilar, L. Jalloul, C. Oestges, and A. Paulraj, "Spatial separation of multi-user MIMO channels," in *IEEE 20th International Symposium on Personal, Indoor and Mobile Radio Communications*, Tokyo, Japan, Sep. 2009, pp. 1059–1063.

[7] G. Dahman, J. Flordelis, and F. Tufvesson, "Experimental evaluation of the effect of bs antenna inter-element spacing on MU-MIMO separation," in *IEEE International Conference on Communications (ICC)*, London, UK, Jun. 2015, pp. 1685–1690.

[8] B. Zhang, Z. Zhong, R. He, B. Ai, G. Dahman, M. Yang, and J. Li, "Multi-user channels with large-scale antenna arrays in a subway environment: Characterization and modeling," *IEEE Access*, vol. 5, pp. 23 613–23 625, 2017.

[9] À. O. Martnez, E. D. Carvalho, and J. Ø. Nielsen, "Towards very large aperture massive MIMO: A measurement based study," in *IEEE Globecom Workshops (GC Wkshps)*, Austin, TX, USA, Dec. 2014, pp. 281–286.

[10] S. Caban, M. Lerch, S. Pratschner, E. Zöchmann, P. Svoboda, and M. Rupp, "Design of experiments to compare base station antenna configurations," *IEEE Transactions on Instrumentation and Measurement*, pp. 1–10, 2018.

[11] C. Masouros and M. Matthaiou, "Space-constrained massive MIMO: Hitting the wall of favorable propagation," *IEEE Communications Letters*, vol. 19, no. 5, pp. 771–774, May 2015.

[12] C. Masouros, C. Jianling, K. Tong, M. Sellathurai, T. Ratnarajah, and W. Junhong, "Large scale antenna arrays with increasing antennas in limited physical space," *China Communications*, vol. 11, no. 11, pp. 7–15, Nov. 2014.

[13] C. Masouros, M. Sellathurai, and T. Ratnarajah, "Large-scale MIMO transmitters in fixed physical spaces: The effect of transmit correlation and mutual coupling," *IEEE Transactions on Communications*, vol. 61, no. 7, pp. 2794–2804, Jul. 2013.

[14] C. Masouros, J. Chen, K. Tong, M. Sellathurai, and T. Ratnarajah, "Towards massive-MIMO transmitters: On the effects of deploying increasing antennas in fixed physical space," in *Future Network Mobile Summit*, Lisboa, Portugal, Jul. 2013, pp. 1–10.

[15] R. Janaswamy, "Effect of element mutual coupling on the capacity of fixed length linear arrays," *IEEE Antennas and Wireless Propagation Letters*, vol. 1, pp. 157–160, 2002.

[16] D. Pinchera, M. D. Migliore, F. Schettino, and G. Panariello, "Antenna arrays for line-of-sight massive MIMO: Half wavelength is not enough," *MDPI Electronics*, vol. 6, no. 3, p. 57, 2017.

[17] S. Pratschner, S. Caban, S. Schwarz, and M. Rupp, "A mutual coupling model for massive MIMO applied to the 3GPP 3D channel model," in *25th European Signal Processing Conference (EUSIPCO)*. Kos, Greece: IEEE, 2017, pp. 623–627.

[18] S. Pratschner, S. Caban, D. Schützenhöfer, M. Lerch, E. Zöchmann, and M. Rupp, "A fair comparison of virtual to full antenna array measurements," in *IEEE International Workshop on Signal Processing Advances in Wireless Communications (SPAWC 2018)*, Kalamata, Greece, Jun. 2018, pp. 1–5.

[19] R. C. Hansen, *Phased array antennas*, 2nd ed. John Wiley & Sons, Dec. 2009.

[20] X. Gao, O. Edfors, J. Liu, and F. Tufvesson, "Antenna selection in measured massive MIMO channels using convex optimization," in *IEEE Globecom Workshops (GC Wkshps)*, Atlanta, GA, USA, Dec. 2013, pp. 129–134.

[21] E. Zöchmann, S. Schwarz, and M. Rupp, "Comparing antenna selection and hybrid precoding for millimeter wave wireless communications," in *IEEE 9th Sensor Array and Multichannel Signal Processing Workshop (SAM 2016)*, Rio de Janeiro, Brazil, Jul. 2016.